




Published by Avanti Publishers
**Journal of Advanced Thermal
Science Research**
ISSN (online): 2409-5826



Thermal-Economic Analysis of an Organic Rankine Cycle System with Direct Evaporative Condenser

Xiaohui Yu ^{*}, Jiabao Geng and Zhi Gao

Hebei Key Laboratory of Thermal Science and Energy Clean Utilization, School of Energy and Environment Engineering, Hebei University of Technology, Tianjin 300401, PR China

ARTICLE INFO

Article Type: Research Article

Academic Editor: S. Pratheesh Kumar 

Keywords:

Economic analysis
Organic rankine cycle
Dynamic performance
Thermodynamic analysis
Direct evaporative condenser

Timeline:

Received: July 05, 2023

Accepted: August 25, 2023

Published: December 20, 2023

Citation: Yu X, Geng J, Gao Z. Thermal-economic analysis of an organic rankine cycle system with direct evaporative condenser. J Adv Therm Sci Res. 2023; 10: 41-58.

DOI: <https://doi.org/10.15377/2409-5826.2023.10.4>

ABSTRACT

The organic Rankine cycle (ORC) system for power generation has proven to be an effective technology for low-temperature waste heat utilization. Accurate prediction and comprehensive comparison of system performance under different conditions are necessary for the development and application of suitable ORC configurations. This paper proposed an organic Rankine cycle (ORC) system using a direct evaporative condenser to realize performance enhancement and analyzed its dynamic performance based on the actual climatic condition, which is beneficial for the performance optimization of this system. This study begins with an introduction to the thermal economics model of the proposed system and evaluates the performance of the system based on the 3E (energy, exergy, economy) analysis method. Secondly, four candidate working fluids were compared and analyzed, leading to the selection of R142b as the best working fluid for the proposed system. Finally, the dynamic performance of the proposed system using the working fluid of R142b was analyzed based on the hourly environment temperature. The result showed that the net thermos-electric conversion efficiency of the system was negatively correlated with the ambient wet-bulb temperature. The annual average exergy efficiency of the system is about 65.79%, and the average exergy loss of the heat absorption unit, evaporative condenser, pump, and expander account for 61.07%, 6.92%, 2.99%, and 29.01% of the exergy loss of the system respectively. In the case 8760 h of operation per year, the payback period of the proposed ORC system using direct evaporative condenser is about 2.14 years.

*Corresponding Author

Emails: 2018133@hebut.edu.cn/ yuxiaohui@tju.edu.cn

Tel: +(86) 226 043 5279

1. Introduction

The increasing serious consumption of fossil fuels has caused a series of problems such as energy shortage and environmental pollution [1, 2]. A good solution is to develop and enhance the utilization of renewable energy like solar energy [3, 4], geothermal energy, wind energy [5, 6], and biomass energy. The other solution is to improve the efficiency of energy conversion and utilization [7, 8]. The evidence shows that the low-temperature waste heat (below 120 °C) from industrial production accounts for about 50% of energy consumption and is not effectively utilized because of technical and economic barriers. Among the possible means of utilizing low-temperature waste heat, the low-temperature power generation system based on organic Rankine cycle (ORC) is considered a well-known promising low-grade thermal-to-power technology [9, 10].

For an ORC system, it is essential to select a suitable working fluid for recovering waste heat. The properties of the working fluid have a significant effect on the performance of the ORC system. Therefore, much research has been conducted on the selection of working fluid [11].

Shahverdi *et al.* [12] developed an energy harvesting system for power generation, investigated the different working fluids in the solar ORC system including R134a, R245ca, R245fa, R152a, R113, R11, and R114b. The test results revealed that R113 had the highest net power, ORC efficiency, and total system efficiency. Kankeyan *et al.* [13] used MATLAB and REFPROP for modeling to evaluate the performance of ORC system with different working fluids. The results showed that R21, R245fa, R123, Neopentane, and R142b have better performance on energy utilization in the range of 50 – 100°C. Ma *et al.* [14] analyzed the nature working fluid and discussed the influence of the physicochemical properties of the working fluid on the thermodynamic properties of the low-temperature organic Rankine cycle. Tchanche *et al.* [15] made a comparative analysis of 20 kinds of working fluids for low-temperature solar ORC systems. Awadh *et al.* [16] conducted a numerical study of a novel solar triplex power generation system by investigating different industrial substances including n-octane, R245fa, R113, R123, cyclohexane, and toluene in the solar ORC system. The results showed that the system can provide the highest electrical energy 152.5 kW using cyclohexane. Song *et al.* [17] simulated a heat pump with an intermediate economizer and the ground source energy drive using EES software and then examined the effect of different parameters on environmental parameters using five working fluids (R134a, R12, R152a, R1234ze(E), and R1234yf).

Some researchers have focused on performance optimization to achieve the optimal performance of the ORC system [18, 19]. Le *et al.* [20] introduced the system efficiency optimization scheme of basic and regenerative supercritical ORCs (organic Rankine cycles) using low-GWP organic compounds as the working fluid. Hou *et al.* [21] proposed a three-level energy efficiency economic evaluation method to evaluate the energy efficiency of the ORC power generation system recovering industrial waste heat. Amirmohammad *et al.* [22] analyzed the proposed combined ORC system from the perspective of thermodynamics and thermoeconomics and compared the performances of different working fluids. Tooli *et al.* [23] conducted a comparative study of different types of supercritical CO₂ integration with ORC using high-temperature heat sources from energy, exergy, and economic (3E) perspectives on different types of supercritical CO₂ integrated ORC using a high-temperature heat source. Xu *et al.* [24] performed a synergistic multi-objective optimization of ORC comprehensive performance under a driving cycle with thermodynamic performance, economic performance, thermoeconomic performance, and environmental impact as optimization objectives. Ashwn *et al.* [25] analyzed the ORC system using environmentally friendly working fluids and optimized its performance using the non-dominated sorting algorithm-II. The results indicate that evaporator temperature and the condenser temperature have a major influence on the ORC's exergetic performance.

For the traditional ORC system, the working fluid is condensed in a condenser, where the heat of the working fluid is transferred to the cooling water. Then, a cooling tower is used to reject the heat to the ambient air. Alternatively, the direct evaporative condenser can be used to directly heat exchange between the working fluid and the ambient air. Compared with the traditional condensing unit of the ORC system, a direct evaporative condenser can reduce the heat transfer area or airflow with the given heat capacity, and enhance heat transfer rate.

Direct evaporative condensers have been widely used to effectively improve the performance of condensing units for the air-conditioning system. Hajidavalloo *et al.* [26] proposed an application of an evaporative-cooled air condenser. The power consumption could be reduced by up to 20% and the coefficient of performance could be improved around 50% at ambient air temperatures from 20 °C to 49 °C. Zhu *et al.* [27] studied experimentally that the heat and mass transfer performance of an evaporative condenser with a horizontal elliptical tube bundle. It was found that the air-wet bulb temperature has greater effects on the heat transfer performance than the air relative humidity. Wei *et al.* [28] designed a vertical tube evaporative condenser to be applied in a small refrigeration system. The COP of the system increased by about 30% compared to the finned tube-type air-cooled condenser. Hayder *et al.* [29] conducted an experimental and theoretical investigation of improving the performance of the conventional air conditioning unit supported by a direct evaporative cooling system. The results show that using evaporative cooling assist enhanced the system to overcome the many challenges by which the refrigeration capacity was increased in the range of 10 – 20%. Beom *et al.* [30] analyzed the energy-saving potential of the air-source heat pump with an evaporative cooler according to the operation strategy. The results show that the proposed system reduces 8.87% of energy consumption compared with the conventional air-source heat pump when the evaporative cooler operates under 72% relative humidity conditions. Venkateswaran *et al.* [31] conducted the experimental testing of the chiller performance of evaporative condensers with the application of jute, cotton, and coconut fiber cooling pads. The results showed that all three cooling pads exhibited enhanced performance in removing heat from the condenser and that jute fiber performed better.

As mentioned above, most of the research focused on the selection of the working fluids and performance optimization for the ORC system. The direct evaporative condenser is a well-known, environmentally friendly method with useful application in the air-conditioning system. However, few studies have ever been done to analyze and evaluate the performance of the ORC system using an evaporative condenser, especially its dynamic performance. This study was inspired by the research gap. Therefore, an ORC system using a direct evaporative condenser to recover low-temperature waste heat (below 120 °C) was proposed, and its dynamic performance was analyzed and discussed based on the hourly environment temperature.

2. System Description

Fig. (1) shows the schematic diagram of the proposed ORC system using a direct evaporative condenser. The proposed ORC system consists of a heat absorption unit (dry pre-heater + flood evaporator), a double screw expander, a working fluid pump, and a direct evaporative condenser.

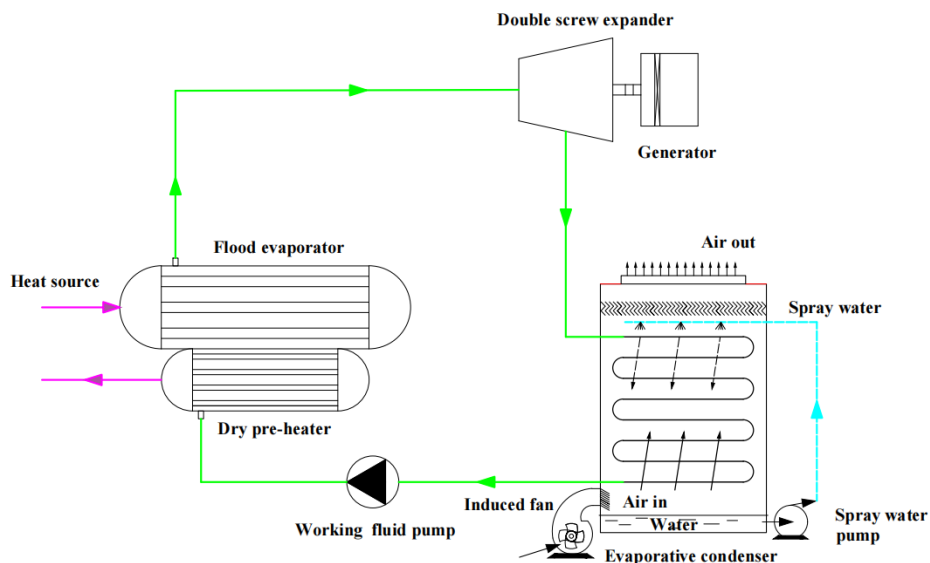


Figure 1: Schematic diagram of the proposed ORC system.

3. Methods

The T-s diagram of the proposed ORC system is depicted in Fig. (2). The ORC consisting of four thermodynamic processes: heat-absorbing process including preheating (2-3), evaporation (3-4) and superheating (4-5), expansion process (5-6), condensation process (6-1) and compression process (1-2). The red and blue lines represent the temperature variable of the heat source and cold source, respectively. For simplified calculation, some assumptions made in this study are listed as follows [32]:

- (1) The pressure loss in the heat exchanger and connecting pipe is ignored.
- (2) Heat transfer loss from the heat exchanger and connecting pipe to the surrounding environment is ignored.
- (3) All components in the system are running under steady state and flow.
- (4) The isentropic efficiency of the expander, circulating water pump, and induced fan are set at a certain value.

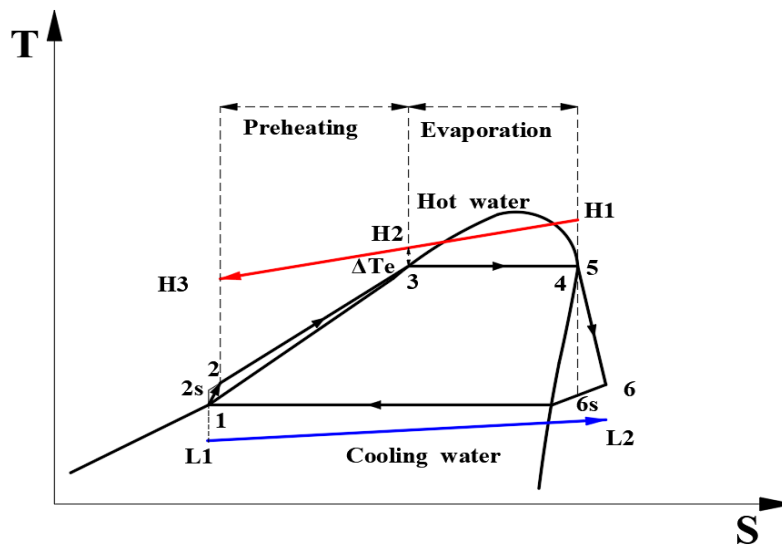


Figure 2: T-s diagrams of the proposed ORC system using direct evaporative condenser.

The flowchart of the presented method is shown in Fig. (3). From Fig. (3), Firstly, the appropriate working fluid for the ORC system is selected. Secondly, the performance parameters of the proposed system are calculated, including the energy index, exergy index, and economic index. Finally, it is applied to a specific case for analysis.

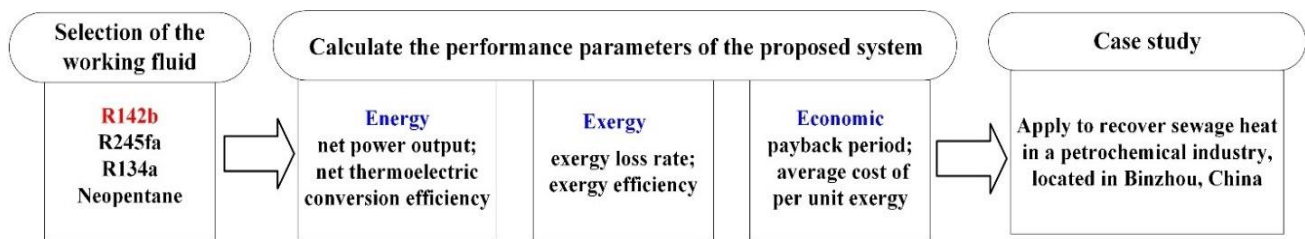


Figure 3: Flowchart of the method.

3.1. Energy Model

The energy equation of each component in the system at a stable steady can be calculated as follows.

3.1.1. Heat Absorption Unit:

The total heat transfer rate can be expressed by the following formula.

$$Q_{pre+eva} = m_w c_{pw} (T_{H1} - T_{H3}) = m_r c_{pr} (T_3 - T_2) + m_r l \quad (1)$$

where c_{pw} is the specific heat capacity of the hot water. T_{H1} and T_{H3} are the inlet and outlet temperatures of the hot water, respectively. l is the latent heat of the working fluid.

The mass flow rate of the working fluid can be calculated as:

$$m_r = m_w c_{pw} (T_{H1} - T_{H3}) / [c_{pr} (T_{evap} - T_{cond}) + l] \quad (2)$$

The latent heat of the working fluid is closely related to its temperature. Thus, the mathematical model proposed by Carruth and Kobayashi is adopted to calculate the latent heat of the working fluid at any temperature [32].

$$l(T) = [7.08(1 - T_r)^{0.345} + 10.95w(1 - T_r)^{0.456}]RT_c/M_r \quad (3)$$

$$w = 3/7[T_{br}/(1 - T_{br})] \ln p_c - 1 \quad (4)$$

where T_c , p_c indicate the critical temperature and critical pressure of the working fluid, respectively. T_r stands for a dimensionless temperature and $T_r = T_{evap}/T_c$. M_r denote the molar mass of the working fluid. w is the acentric factor. T_{br} is a dimensionless temperature in which $T_{br} = T_b/T_c$.

The c_{pr} in Eqs. (1) and (2) are usually affected by the temperature but not the pressure, which expressed as:

$$c_{pr}(T) = a + bT + cT^2 + dT^3 \quad (5)$$

where the coefficients a , b , c , d can be obtained by fitting data. They are obtained based on the data of REFPROP 9.1 in this study.

3.1.2. Expander:

The energy balance equation of the expander can be expressed as [33, 34]:

$$W_{E,g} = \eta_{E,S} m_r (h_5 - h_{6s}) \quad (6)$$

where $W_{E,g}$ is the shaft work of the expander. $\eta_{E,S}$ denotes the isentropic efficiency of the double screw expander, where is assumed at 0.8.

3.1.3. Working Fluid Pump:

The power input of the working fluid pump can be calculated as [35]:

$$W_{FP} = m_r (h_2 - h_1) \quad (7)$$

3.1.4. Direct Evaporative Condenser:

The evaporative condenser mainly includes three parts: heat exchanger coil system, water cycle system, and fan. The model of the evaporative condenser was built by making the following assumptions [36]:

- (1) The water film temperature along the height of the evaporative condenser is not considered.
- (2) The evaporated quantity of the cooling water is ignored.
- (3) Only the heat transfer of working fluid during condensation in the evaporative condenser tube is considered.
- (4) The heat transfer coefficient in the evaporative condenser is constant.

The energy transfer rate of the direct evaporative condenser can be calculated as:

$$Q_{cond} = m_f(h_6 - h_1) \quad (8)$$

The heat transfer in the evaporative condenser consists of two parts: (1) the heat transfer from the high-temperature and pressure gaseous working fluid to the water film. (2) the heat transfer between water film and air. The quantity of the heat transferred from condensing working fluid to water film is expressed as:

$$Q_{f-w} = K_{f-w}(T_{cond} - T_w)A_0 \quad (9)$$

where T_w is the average surface temperature of the water film. K_{f-w} denotes the coefficient of heat transfer and A_0 is the heat exchange area of the tube in the evaporative condenser.

The second phase of the heat transfer between the water film and the air can be calculated as:

$$Q_{w-a} = h_w A_0 (T_a - T_w) = K_{w-a} A_0 (w_w - w_a) h_{fg} \quad (10)$$

Radiation heat transfer is small and neglected in this study [36]. Consequently, $Q_{cond} = Q_{f-w} = Q_{w-a}$.

The power consumption of the fan and circulating water pump in the direct evaporative condenser can be obtained by referring to the empirical formula.

The power consumption of the fan can be calculated as:

$$N_f = \Delta P L_d Q_{cond} = 9.28 Q_{cond} \quad (11)$$

The power consumption of the circulating water pump can be calculated as:

$$N_s = 9.8 G_s H_z Q_{cond} = 1.69 Q_{cond} \quad (12)$$

where L_d is the combustion air volume and assumed to be 0.03. G_s is the water flow corresponding to per condensing load and here is 0.018. H_z is the pump head and is assumed to be 10 m.

The performance of the ORC power generation on system using direct evaporative condenser can be evaluated by the following thermodynamic indexes.

The net power output of the proposed system can be defined as [37]:

$$W_{net} = W_{E,g} - W_{FP} - N_s - N_f \quad (13)$$

The net thermoelectric conversion efficiency of the proposed system can be defined as:

$$\eta_{net} = W_{net} / Q_{evap} \quad (14)$$

3.2. Exergy Model

To quantitatively analyze the cause of the imperfect thermodynamic process, the exergy model of the proposed ORC system is built according to the first and second laws of thermodynamics.

The exergy rate balance can be calculated as:

$$\sum Ex_{in} = \sum Ex_{out} + W + L \quad (15)$$

where L is the exergy loss rate.

The exergy rate of the fluid at each state point can be calculated as [38]:

$$Ex = m_r[(h - h_0) - T_0(s - s_0)] \quad (16)$$

For the fluid with variable temperature in the component, the exergy rate can be calculated [38]:

$$Ex_Q = Q(1 - T_0/T_h) \quad (17)$$

The exergy rate balance equation and the exergy efficiency for each component of the proposed system are indicated in Table 1.

Table 1: The exergy rate balance equation and the exergy efficiency for each component.

Component	Exergy Rate Balance Equation	Exergy Efficiency
Evaporator	$L_{evap} = EX_2 + EX_{Q_{evap}} - EX_5$	$\psi_{evap} = (EX_5 - EX_2) / EX_{Q_{evap}}$
Working fluid Pump	$L_{FP} = EX_1 + W_{FP} - EX_2$	$\psi_{FP} = (EX_2 - EX_1) / W_{FP}$
Expander	$L_E = EX_5 - EX_6 - W_E$	$\psi_E = W_E / (EX_5 - EX_6)$
Evaporative condenser	$L_{cond} = EX_6 - EX_1 - EX_{Q_{cond}}$	$\psi_{cond} = EX_{Q_{cond}} / (EX_6 - EX_1)$

The exergy efficiency of the proposed system can be defined as:

$$\psi_{sys} = [Ex_{Q_{evap}} - (L_{evap} + L_{FP} + L_E + L_{cond})] / Ex_{Q_{evap}} \quad (18)$$

3.3. Economic Model

Expansion machine, working fluid pump and heat exchanger (evaporator and direct evaporative condenser) are the most important components of the proposed system. The unit cost of exergy for the product is used to assess the economic performance of the proposed system.

The average unit exergy cost of the proposed system is defined as [39]:

$$c_{product} = C_{product} / W_{net} \quad (19)$$

where $C_{product}$ is the product cost rate and can be calculated as:

$$C_{product} = C_{fuel} + \sum(Z_i + Z_{op}) \quad (20)$$

$$Z_i + Z_{op} = \varphi Z_c \cdot CRF / (N \cdot 3600) \quad (21)$$

where C_{fuel} is the fuel cost rate and Z_c denotes the capital investment cost of each component that can be estimated based on the cost functions listed in Table 2. CRF (capital recovery factor) can be expressed as [40]:

$$CRF = i \cdot (1 + i)^n / [(1 + i)^n - 1] \quad (22)$$

The heat transfer area of the heat exchange unit can be calculated as:

$$A_{evap} = Q_{evap} / (KF_{lm} \Delta T_{lm}) \quad (23)$$

where K and ΔT_{lm} represent the total heat transfer coefficient and the logarithmic average temperature difference of the heat exchanger, respectively. F_{lm} is the logarithmic average temperature difference correction coefficient [41].

As one of the capital budget indicator, the payback period (PBP) of the proposed ORC system can be calculated as:

$$PBP = C_{product} \cdot 3600n / (W_{net} \cdot EP) \quad (24)$$

Table 2: Capital investment cost function of each component.

Component	Capital Cost Function (Z_c)	Ref.
Heat absorption unit	$1397 \cdot A_{evap}^{0.89}$	[40]
Direct evaporative condenser	$4430 \cdot (0.1 V_c)^{0.63}$	[42]
Pump	$1970 \cdot W_{FP}^{2.35}$	[43]
Expander	$4405 \cdot W_e^{1.7}$	[44]

Table 3: Specific values of the parameters used in economic analysis [41, 45, 46].

Parameters	Value
Maintenance factor, φ	1.06
Annual interest rate, i (%)	7.5
The system lifetime, n (yr)	15
Average annual operating time of ORC system, N (h)	8760
Average of electricity price for China, EP \$(/kW·h)	0.11

4. Case Study

For the sake of practicability and credibility, the proposed system was used to recover sewage heat in a petrochemical industry, located in Binzhou, China. The specific experimental device is shown in Fig. (4). The actual operating data of the sewage heat were collected and applied for the performance analysis in this study. Table 4 presents the design conditions of the proposed ORC power generation system using direct evaporative condenser.

**Figure 4:** Picture of ORC system engineering case.**Table 4: Design conditions of the proposed ORC power generation system.**

Parameters	Value
Sewage temperature, ($^{\circ}\text{C}$)	110
Mass flow rate of the sewage, (t/h)	80
Evaporation temperature, T_{evap} ($^{\circ}\text{C}$)	80
Pinch point temperature difference in the heat absorption unit, ΔT_e ($^{\circ}\text{C}$)	10
Temperature of the outlet water to the heat absorption unit, ($^{\circ}\text{C}$)	75
Temperature of the inlet water to the dry pre-heater, ($^{\circ}\text{C}$)	90

The selection of the working fluids exhibits a significant effect on the thermo-economic performance of the ORC system. Therefore, a suitable working fluid can improve the thermodynamic efficiency and reduce the investment cost of the ORC system. Table (5) summarizes the recommended working fluids for the ORC system using low-temperature heat energy. R142b, R245fa, R134a, and Neopentane were chosen as the candidate working fluids for the proposed system from the recommended working fluids in Table 5.

Table 5: Recommended working fluids for low-temperature heat source [41,47–50].

Applications	Heat-Source Temperature	Performance Indicators	Recommended Fluids
-	70 – 110 °C	-	R142b, Neopentane
Waste heat recovery	50 – 280 °C	Net power output	R245fa, R141b
Waste heat recovery	85 °C	Thermal efficiency	R245fa
Solar energy	60 – 100 °C	Second law efficiency Total irreversibility	R134a
Waste heat recovery	120 °C	First law efficiency Power output Second law efficiency Electricity cost	R134a, isobutane

5. Results and Discussion

5.1. Model Validation

To verify the feasibility and reliability of the proposed model, it was used to evaluate the net output power of the proposed ORC system compared with our tested data for the proposed ORC system in practical engineering. The tested data was collected under different cold source temperatures in the range of 15 – 30 °C. The comparison results between our tested data and the simulated net output power of the ORC system by the proposed model are shown in Fig. (5). According to Fig. (5), the simulation result with a decrease in the condensation temperature agrees well with the tested results. The maximum relative difference between simulated and tested data is less than 7.86 %. Therefore, that the feasibility and reliability of the proposed model are verified based on the comparison results.

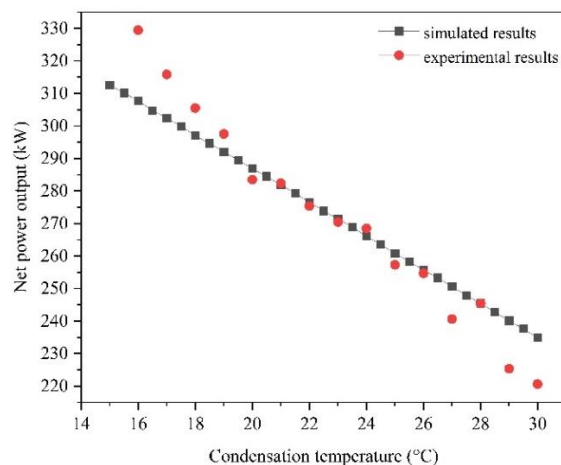


Figure 5: Comparison of net output power versus condensing temperature.

5.2. Working Fluid Selection

Fig. (6) shows the thermo-economic performance of the proposed ORC system using several candidate working fluids under the design condition considering the variable environmental temperature.

The variation of net power output with condensation temperature is given in Fig. (6a). The net power output of the proposed system using different working fluids proportionally decreases with the condensation temperature under a given evaporating temperature. According to Fig. (6a), R142b has the highest net output power, followed by R245fa, Neopentane, and R134a. The net output power of the proposed system using R142b drops by 77.79 kW when the condensation temperature rises from 15 to 30 °C. The variation of the net thermoelectric conversion efficiency of the proposed ORC system with the condensation temperature is shown in Fig. (6b). With the condensation temperature increases from 15 to 30 °C, the net thermoelectric conversion efficiency of the system decreased by 2.39%, 2.36%, 2.15% and 2.30% for R142b, R245fa, R134a and Neopentane, respectively. The system of R142b has the largest net thermoelectric conversion efficiency, and the system with R245fa is following closely.

From Fig. (6c), the exergy efficiency of the system under each proposed working fluid also showed obvious differences. The result indicates that the exergy efficiency of system with R142b and R245fa is much higher than that of R134a and Neopentane under the same condensation temperature. The exergy efficiency of system with R142b is slightly higher than that of R245fa under the condensation temperature of 15 - 22 °C. Fig. (6d) illustrates the variation of the average cost per unit exergy with condensation temperature. The average cost per unit exergy increases with the increase of the condensation temperature for different working fluids. The system with R142b has the lowest average cost per unit exergy, and the system with R245fa is the following.

Table 6 gives the system performance of different working fluids. The results show that the system using R142b as a working fluid has good thermodynamic performance and a low average cost per unit exergy. Therefore, R142b is selected as the most suitable working fluid for the proposed ORC system.

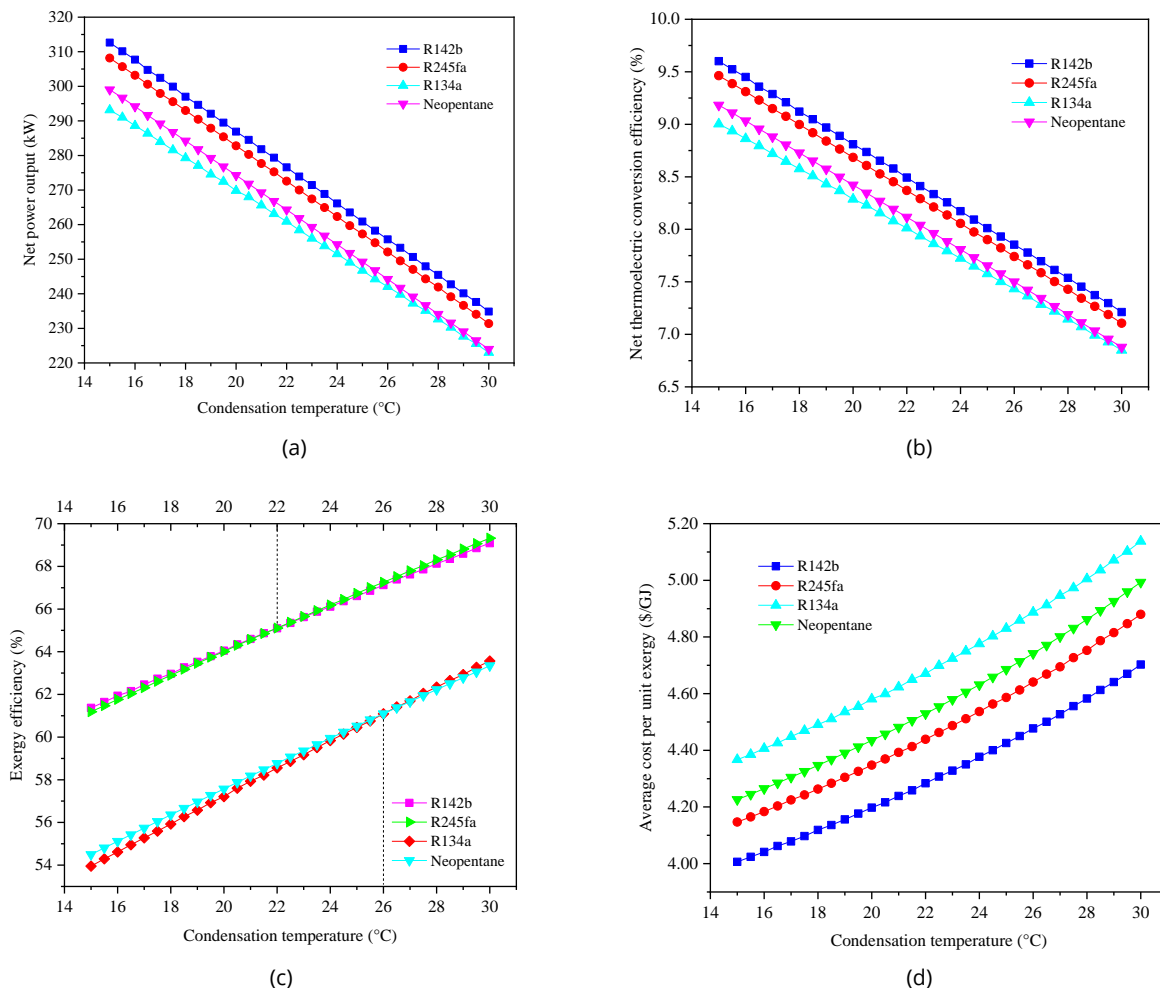


Figure 6: Performance analysis of several candidate working fluids in the proposed ORC system.

Table 6: Comparison of the proposed system performance using different working fluids.

-	Average Net Thermoelectric Conversion Efficiency (%)	Average Net Power Output (kW)	Average Exergy Efficiency (%)	Annual Average Cost Per Unit Exergy (\$/GJ)
R142b	8.25	268.78	65.79	4.381
R245fa	8.13	264.89	65.84	4.542
Neopentane	7.88	256.70	59.43	4.639
R134a	7.79	253.62	59.56	4.782

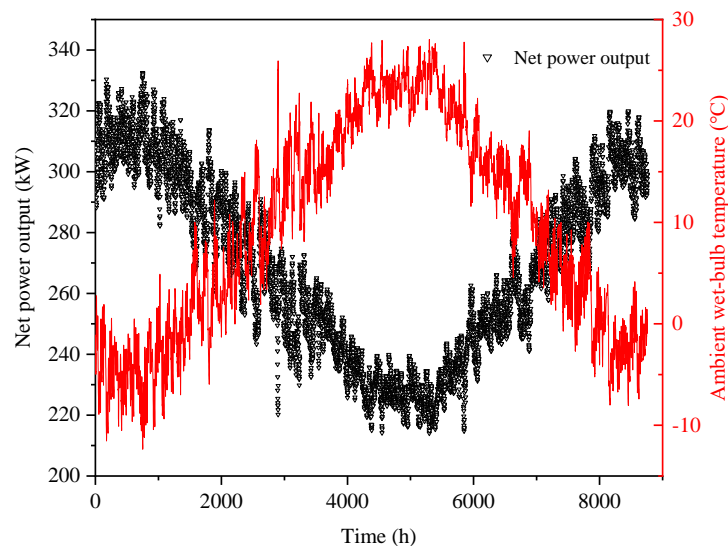
5.3. Dynamic Performance Analysis Results

Compared with traditional ORC power generation systems, the proposed ORC system using direct evaporative condensers is sensitive to the ambient conditions (temperature and humidity). For the practical case, the ambient condition varies with time. Thus, the annual dynamic thermo-economic performance of the proposed ORC system using R142b was investigated and analyzed based on hourly data for the environmental conditions. The typical meteorological year data of Binzhou was chosen to analyze the annual dynamic performance of the presented ORC system using a direct evaporative condenser.

5.3.1. Energetic Analysis Result

Fig. (7) shows the variation of the net power output with time. It can be seen that the net power output has an opposite trend to the ambient wet-bulb temperature. The net power output decreases from 332.56 kW to 214.06 kW as the ambient wet-bulb temperature varies from -12.3 °C to 28.0 °C. Every 1 °C increase in ambient wet-bulb temperature can cause about a 3.95 kW decrease in the net power output. The variation of the net thermoelectric conversion efficiency with ambient wet-bulb temperature is shown in Fig. (8). It can be seen that the energy efficiency of the proposed ORC system is also negatively correlated with the air wet-bulb temperature. The net thermoelectric conversion efficiency of the system can reach the highest close to 10%. The net thermoelectric conversion efficiency drops to be lowest of about 6.57% with the air wet-bulb temperature reaches 28.03 °C.

The analysis results show that the air wet-bulb temperature has a great influence on the energy performance of the proposed system using the direct evaporative condenser. This is because the temperature lift increases as the ambient wet-bulb temperature decreases. High enthalpy difference and temperature lifts result in a high net power generation and net thermoelectric conversion efficiency.

**Figure 7:** Variation of the net power output of the system with the ambient wet-bulb temperature.

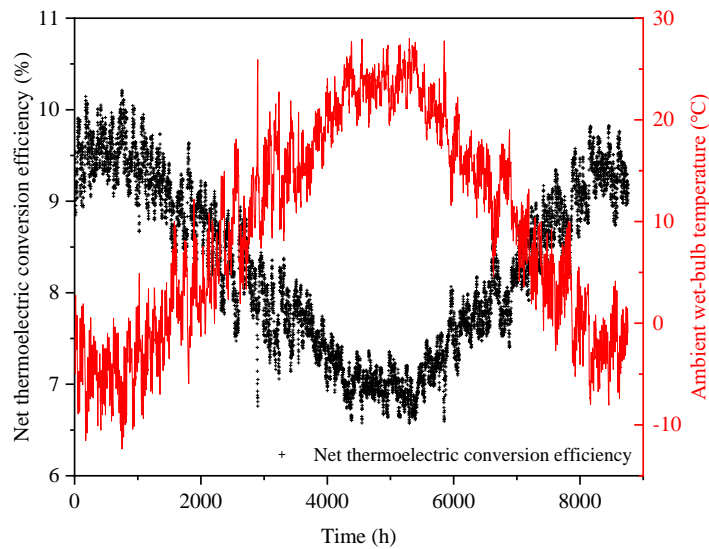
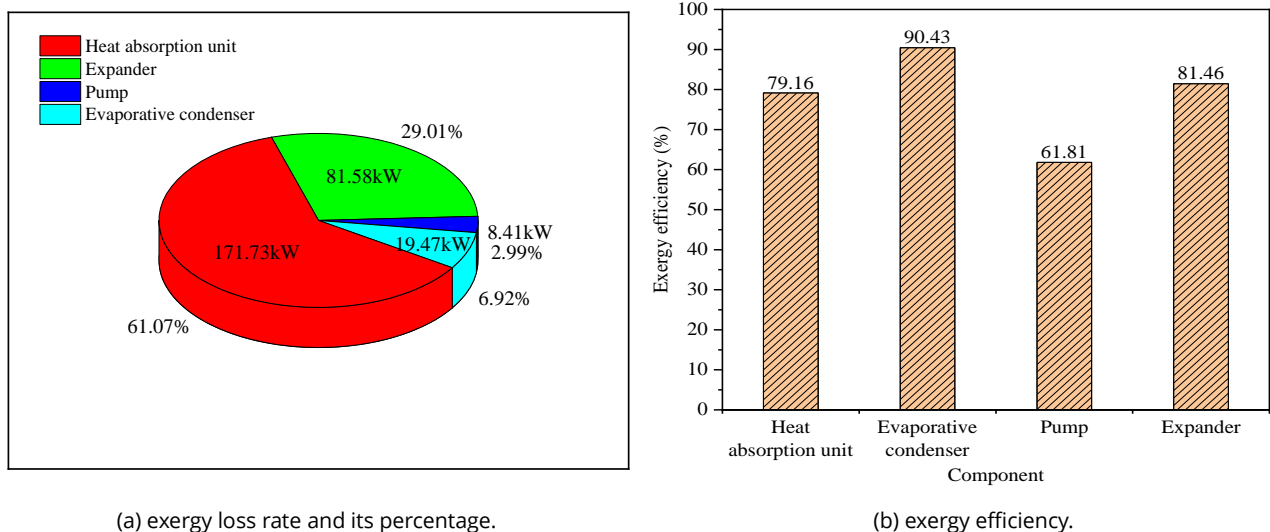


Figure 8: Variation of the net thermoelectric conversion efficiency of the proposed system with the ambient wet-bulb temperature.

5.3.2. Exergy Analysis Result

Fig. (9) shows the average exergy loss rate and exergy efficiency of each component in the proposed ORC system. Fig. (9a) reveals that the heat absorption unit exhibits the largest exergy loss rate, which amounts to 171.73 kW, followed by the expander (81.58 kW) and direct evaporative condenser (19.47 kW). As shown in Fig. (9b), the working fluid pump has the lowest exergy efficiency of 61.81% and the heat absorption unit has low exergy efficiency of 79.16%. Thus, the heat absorption unit has great potential for reducing the exergy loss rate and improving noticeably the exergy efficiency of the proposed ORC system.



(a) exergy loss rate and its percentage.

(b) exergy efficiency.

Figure 9: (a) Average exergy loss rate and its percentage of each component. (b) Average exergy efficiency of each component under annual operating condition.

Fig. (10) shows the exergy efficiency variation of the proposed ORC system with time in the typical year. Obviously, as the ambient air wet-bulb temperature increase, the exergy efficiency of the proposed system increases. It can be seen that the exergy efficiency of the system is in the range of 50.23% – 70.95% with the ambient air wet-bulb temperature of -12.36°C – 28.03°C. This is mainly because the high environmental wet-bulb temperature and condensation temperature lead to a reduction in the entropy difference of each component, which is the decisive factor of the exergy loss and exergy efficiency for a given evaporation temperature.

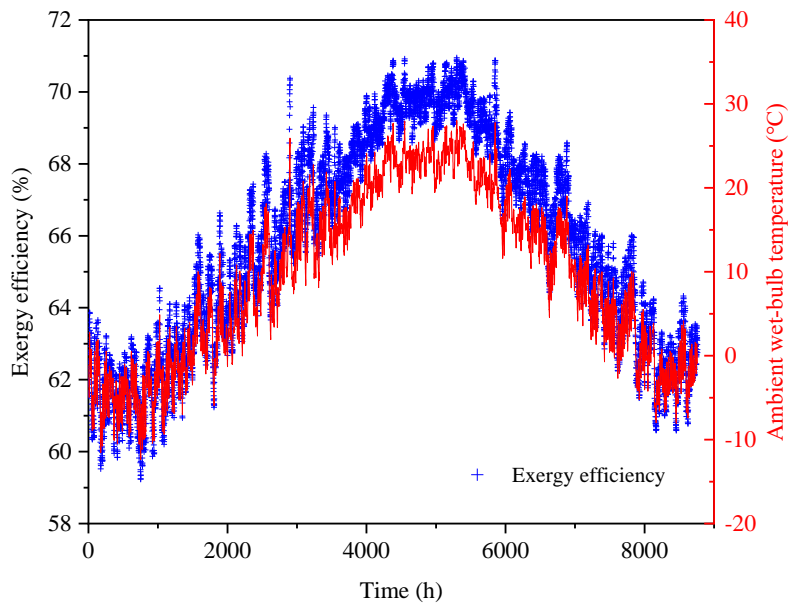


Figure 10: Variation of the exergy efficiency of the proposed ORC system with time.

5.3.3. Economic Analysis Result

From Fig. (11), the unit exergy cost of the system increases gradually as the increases of air wet-bulb temperature. The results of regression analysis suggest that there is a good polynomial correlation between these two parameters. The unit exergy cost increased from 3.88 \$/GJ to 4.97 \$/GJ when the air wet-bulb temperature increased from -12.36 to 28.06°C. *PBP* is one of the important factors in the feasibility analysis for practical engineering. Fig. (12) shows the *PBP* variation of the proposed system with the condensation temperature. The *PBP* increases with the increase of the ambient air wet-bulb temperature. The presented ORC system using a direct evaporative condenser in the case shows good economic performance and the payback period is about 2.14 years based on the hourly environment temperature in the typical year.

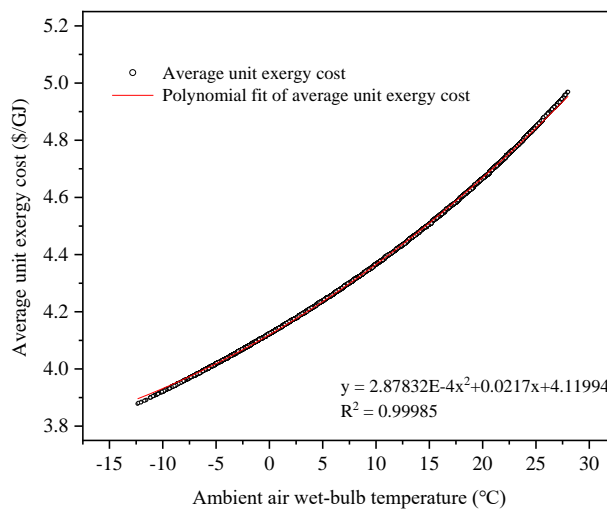


Figure 11: Variation of the average cost per unit exergy with the ambient air wet-bulb temperature.

5.3.4. Comparison of Results

Table (7) gives the results of the comparison of the simulated data with the data from the existing literature. By comparison, the net output power of this system is increased by 51.70 kW, the exergy efficiency is increased by 20.97%, and the payback period is reduced by 0.03 years.

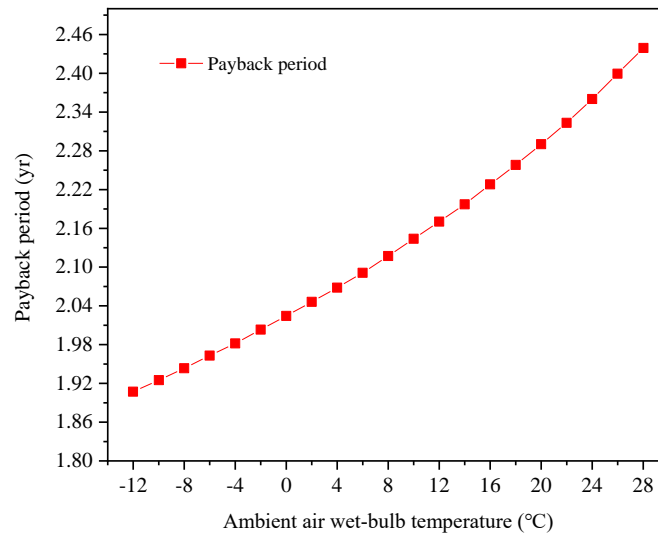


Figure 12: Variation of the payback period with the ambient air wet-bulb temperature.

Table 7: Comparison of simulated data with existing studies.

Types	Simulation Data	Comparative Data [40]
Net power output, (kW)	286.88	235.18
Exergy efficiency, (%)	67.23	46.26
Payback period, (yr)	2.29	2.32

6. Conclusions and Outlook

This paper introduces an ORC power generation system using a direct evaporative condenser, to recover low-temperate heat energy. The 3E (energy, exergy, economy) analysis method was used to compare and analyze the thermal-economics performance of the proposed system using different working fluids based on a case located in Binzhou, Shandong province, China. In addition, the dynamic performance of the proposed ORC system was investigated based on the hourly ambient temperature in the typical year. The main conclusions are as follows:

1. Compared with the other three candidate working fluids, R142b is the best working fluid for the proposed system. The impact of a mixture of working fluids on the ORC systems could be considered in the follow-up work.
2. The heat absorption unit and pump in the proposed system need to be improved in terms of their exergy performance. The exergy loss rate (117.73 kW) of the heat absorption unit is the largest and the exergy efficiency (61.81%) of the pump is the lowest measured in the system.
3. The air-wet bulb temperature has a great influence on the energy performance and the average unit exergy cost of the proposed ORC system. The presented ORC system using a direct evaporative condenser in the case shows good economic performance and the payback period is about 2.14 years. The effect of factors such as system layout on system performance can be investigated to optimize the system in the follow-up work.

Nomenclature

h	specific enthalpy (kJ/kg)
Q	heat transfer rate (kW)

W	work output (kW)
L	exergy loss rate (kW)
E_x	exergy rate (kW)
s	specific entropy [kJ/(kg·K)]
φ	maintenance factor
Z_i	capital cost rate
Z_{op}	maintenance cost rate
N	annual operating hour (h)
K	heat transfer coefficient [W/(m ² ·K)]
ΔP	pressure loss (Pa)
h_{fg}	Latent heat of vaporization (kJ/kg)
PBP	payback period
ORC	organic Rankine cycle
CRF	capital recovery factor
η_E	generator efficiency (%)
ψ	exergy efficiency (%)
T	temperature(K)

Subscript

h	heat source
net	net power output
r	working fluid
$cond$	evaporative condenser
$evap$	Evaporator
sys	System
0	environmental condition
E	expander
FP	working fluid pump

Conflict of Interest

The authors declare that they have no known competing financial interests or personal relationships that could have appeared to influence the work reported in this paper.

Funding

This research was supported by the National Key R&D Program of China (No. 2022YFE0208300).

Authors' Contribution

Xiaohui Yu: Formal analysis, Funding acquisition, Writing – review & editing, Conceptualization. **Jiabao Geng:** Writing – original draft, Investigation, Methodology, Data curation. **Zhi Gao:** Writing – review, Methodology, Data curation.

References

- [1] Mahmoudi A, Fazli M, Morad MR. A recent review of waste heat recovery by organic rankine cycle. *Appl Therm Eng.* 2018; 143: 660-75. <https://doi.org/10.1016/j.applthermaleng.2018.07.136>
- [2] Singh AK, Samsher. Techno-environ-economic-energy-exergy-matrices performance analysis of evacuated annulus tube with modified parabolic concentrator assisted single slope solar desalination system. *J Clean Prod.* 2022; 332: 129996. <https://doi.org/10.1016/j.jclepro.2021.129996>
- [3] Singh AK. An inclusive study on new conceptual designs of passive solar desalting systems. *Heliyon.* 2021; 7(2): E05793. <https://doi.org/10.1016/j.heliyon.2020.e05793>
- [4] Singh AK. Mathematical analysis of optimized requisites for novel combination of solar distillers. *J Eng Res.* 17 June 2023 [In press]. <https://doi.org/10.1016/j.jer.2023.100121>
- [5] Srivastava BK, Shankar V, Singh AK. Low-speed wind power generation system: An overview. *Lecture Notes in Mechanical Engineering*, Singapore: Springer; 2023, p. 189-98. https://doi.org/10.1007/978-981-19-3498-8_17
- [6] Singh AK, Kumar P, Kishore R, Singh P, Kant N, Singh P, *et al.* Stumpy-paced green power generation system. 2021 4th International Conference on Recent Developments in Control, Automation & Power Engineering (RDCAPE), Noida: IEEE; 2021, p. 351-5. <https://doi.org/10.1109/RDCAPE52977.2021.9633633>
- [7] Singh AK, Gautam S. Optimum techno-eco performance requisites for vacuum annulus tube collector-assisted double-slope solar desalination unit integrated modified parabolic concentrator. *Environ Sci Pollut Res.* 2022; 29: 34379-405. <https://doi.org/10.1007/s11356-021-18426-x>
- [8] Romero RJ, Cerezo J, Rodríguez Martínez A, Hernández Luna G, Montiel Gutiérrez M. On the dimensionless absorption heat pump widespread. *J Adv Therm Sci Res.* 2021;8:10–20. <https://doi.org/10.15377/2409-5826.2021.08.2>
- [9] Luo X, Liang Z, Guo G, Wang C, Chen Y, Ponce-Ortega JM, *et al.* Thermo-economic analysis and optimization of a zoetroptic fluid organic Rankine cycle with liquid-vapor separation during condensation. *Energy Convers Manag.* 2017; 148: 517-32. <https://doi.org/10.1016/j.enconman.2017.06.002>
- [10] Yan L, Liu J, Ying G, Zhang N. Simulation analysis of flue gas waste heat utilization retrofit based on ORC system. *Energy Eng.* 2023; 120: 1919-38. <https://doi.org/10.32604/ee.2023.027546>
- [11] Arjunan P, Gnana Muthu JH, Somanasari Radha SL, Suryan A. Selection of working fluids for solar organic rankine cycle—A review. *Int J Energy Res.* 2022; 46: 20573-99. <https://doi.org/10.1002/er.7723>
- [12] Shahverdi K, Loni R, Ghobadian B, Monem MJ, Gohari S, Marofi S, *et al.* Energy harvesting using solar ORC system and Archimedes Screw Turbine (AST) combination with different refrigerant working fluids. *Energy Convers Manag.* 2019; 187: 205-20. <https://doi.org/10.1016/j.enconman.2019.01.057>
- [13] Thurairaja K, Wijewardana A, Jayasekara S, Ranasinghe C. Working fluid selection and performance evaluation of ORC. *Energy Procedia.* 2019; 156: 244-8. <https://doi.org/10.1016/j.egypro.2018.11.136>
- [14] Ma W, Liu T, Min R, Li M. Effects of physical and chemical properties of working fluids on thermodynamic performances of medium-low temperature organic Rankine cycles (ORCs). *Energy Convers Manag.* 2018; 171: 742-9. <https://doi.org/10.1016/j.enconman.2018.06.032>
- [15] Tchanche BF, Papadakis G, Lambrinos G, Frangoudakis A. Fluid selection for a low-temperature solar organic Rankine cycle. *Appl Therm Eng.* 2009; 29: 2468-76. <https://doi.org/10.1016/j.applthermaleng.2008.12.025>
- [16] Almohammadi BA, Al-Zahrani A, Refaey HA, Attia E-A, Fouda A. Energy analysis of a novel solar tri-generation system using different ORC working fluids. *Case Stud Therm Eng.* 2023; 45: 102918. <https://doi.org/10.1016/j.csite.2023.102918>
- [17] Zhao S, Abed AM, Deifalla A, Al-Zahrani A, Aryanfar Y, García Alcaraz JL, *et al.* Competitive study of a geothermal heat pump equipped with an intermediate economizer for various ORC working fluids. *Case Stud Therm Eng.* 2023; 45: 102954. <https://doi.org/10.1016/j.csite.2023.102954>
- [18] Yang F, Zhang H, Song S, Bei C, Wang H, Wang E. Thermo-economic multi-objective optimization of an organic rankine cycle for exhaust waste heat recovery of a diesel engine. *Energy.* 2015; 93: 2208-28. <https://doi.org/10.1016/j.energy.2015.10.117>
- [19] Manfredi M, Spinelli A, Astolfi M. Definition of a general performance map for single stage radial inflow turbines and analysis of the impact of expander performance on the optimal ORC design in on-board waste heat recovery applications. *Appl Therm Eng.* 2023; 224: 119857. <https://doi.org/10.1016/j.applthermaleng.2022.119857>
- [20] Le VL, Feidt M, Kheiri A, Pelloux-Prayer S. Performance optimization of low-temperature power generation by supercritical ORCs (organic Rankine cycles) using low GWP (global warming potential) working fluids. *Energy.* 2014; 67: 513-26. <https://doi.org/10.1016/j.energy.2013.12.027>
- [21] Hou Z, Wei X, Ma X, Meng X. Exergoeconomic evaluation of waste heat power generation project employing organic rankine cycle. *J Clean Prod.* 2020; 246: 119064. <https://doi.org/10.1016/j.jclepro.2019.119064>
- [22] Behzadi A, Gholamian E, Houshfar E, Habibollahzade A. Multi-objective optimization and exergoeconomic analysis of waste heat recovery from Tehran's waste-to-energy plant integrated with an ORC unit. *Energy.* 2018; 160: 1055-68. <https://doi.org/10.1016/j.energy.2018.07.074>

- [23] Tooli A, Fallah M, Mosaffa AH. A comparative study on the integration of different types of supercritical CO₂ with ORC using high-temperature heat source from energy, exergy, and exergoeconomic (3E) viewpoint. *J Braz Soc Mech Sci Eng.* 2023; 45: Article number: 366. <https://doi.org/10.1007/s40430-023-04281-z>
- [24] Ping X, Yang F, Zhang H, Xing C, Pan Y, Yang H, *et al.* A synergistic multi-objective optimization mixed nonlinear dynamic modeling approach for organic Rankine cycle (ORC) under driving cycle. *Appl Therm Eng.* 2023; 228: 120455. <https://doi.org/10.1016/j.applthermaleng.2023.120455>
- [25] Ashwni NA, Sherwani AF. Exergy analysis and multi-objective optimisation of ORC using NSGA-II. *Int J Exergy.* 2023; 40: 130-43. <https://doi.org/10.1504/IJEX.2023.128775>
- [26] Hajidavalloo E, Eghtedari H. Performance improvement of air-cooled refrigeration system by using evaporatively cooled air condenser. *Int J Refrig.* 2010; 33: 982-8. <https://doi.org/10.1016/j.ijrefrig.2010.02.001>
- [27] Junior ICA, Smith-Schneider P. Consolidated experimental heat and mass transfer database for a reduced scale evaporative condenser. *Int J Refrig.* 2016; 66: 21-31. <https://doi.org/10.1016/j.ijrefrig.2015.12.006>
- [28] Wei J, Liu J, Xu X, Ruan J, Li G. Experimental and computational investigation of the thermal performance of a vertical tube evaporative condenser. *Appl Therm Eng.* 2019; 160: 114100. <https://doi.org/10.1016/j.applthermaleng.2019.114100>
- [29] Hashim RH, Hammdi SH, Eidan AA. Enhancement of air conditioning system using direct evaporative cooling: Experimental and theoretical investigation. *Open Eng.* 2023; 13: 20220415. <https://doi.org/10.1515/eng-2022-0415>
- [30] Kim B-J, Jo S-Y, Jeong J-W. Energy performance enhancement in air-source heat pump with a direct evaporative cooler-applied condenser. *Case Stud Therm Eng.* 2022; 35: 102137. <https://doi.org/10.1016/j.csite.2022.102137>
- [31] Naveenprabhu V, Suresh M. Performance studies on a water chiller equipped with natural fiber cooling pad based evaporative condenser. *Ind Crops Prod.* 2023; 201: 116923. <https://doi.org/10.1016/j.indcrop.2023.116923>
- [32] Dong S, Zhang Y, He Z, Yu X, Zhang Y, Kong X. Optimum design method of organic rankine cycle system based on semi-empirical model and experimental validation. *Energy Convers Manag.* 2016; 108: 85-95. <https://doi.org/10.1016/j.enconman.2015.10.083>
- [33] Fernández FJ, Prieto MM, Suárez I. Thermodynamic analysis of high-temperature regenerative organic Rankine cycles using siloxanes as working fluids. *Energy.* 2011; 36: 5239-49. <https://doi.org/10.1016/j.energy.2011.06.028>
- [34] Zhang X, Bai H, Zhao X, Diabat A, Zhang J, Yuan H, *et al.* Multi-objective optimisation and fast decision-making method for working fluid selection in organic Rankine cycle with low-temperature waste heat source in industry. *Energy Convers Manag.* 2018; 172: 200-11. <https://doi.org/10.1016/j.enconman.2018.07.021>
- [35] Hu K, Zhang Y, Yang W, Liu Z, Sun H, Sun Z. Energy, exergy, and economic (3E) analysis of transcritical carbon dioxide refrigeration system based on ORC system. *Energies (Basel).* 2023; 16(4): 1675. <https://doi.org/10.3390/en16041675>
- [36] Meng Z, Meng Z, Lu W, Zhu Z, Sun Y. Research on heat exchange and control method of the evaporative condenser in the equipment of flax fiber modification. *Appl Therm Eng.* 2016; 100: 595-601. <https://doi.org/10.1016/j.applthermaleng.2016.02.011>
- [37] Bu S, Yang X, Li W, Su C, Dai W, Wang X, *et al.* Energy, exergy, exergoeconomic, economic, and environmental analyses and multiobjective optimization of a SCMR-ORC system with zeotropic mixtures. *Energy.* 2023; 263: 125854. <https://doi.org/10.1016/j.energy.2022.125854>
- [38] Jiang Y, Zhan L, Tian X, Nie C. Thermodynamic performance comparison and optimization of sCO₂ brayton cycle, tCO₂ brayton cycle and tCO₂ rankine cycle. *J Therm Sci.* 2023; 32: 611-27. <https://doi.org/10.1007/s11630-023-1708-z>
- [39] Wu Z, Sha L, Zhao M, Wang X, Ma H, Zhang Y. Performance analyses and optimization of a reverse carnot cycle-organic Rankine cycle dual-function system. *Energy Convers Manag.* 2020; 212: 112787. <https://doi.org/10.1016/j.enconman.2020.112787>
- [40] Harby K, Gebaly DR, Koura NS, Hassan MS. Performance improvement of vapor compression cooling systems using evaporative condenser: An overview. *Renew Sustain Energy Rev.* 2016; 58: 347-60. <https://doi.org/10.1016/j.rser.2015.12.313>
- [41] Yao S, Zhang Y, Yu X. Thermo-economic analysis of a novel power generation system integrating a natural gas expansion plant with a geothermal ORC in Tianjin, China. *Energy* 2018;164:602-14. <https://doi.org/10.1016/j.energy.2018.09.042>
- [42] Marcello S. On the exergoeconomic assessment of employing Kalina cycle for GT-MHR waste heat utilization. *Energy Convers Manag.* 2015; 90: 364-74. <https://doi.org/10.1016/j.enconman.2014.11.039>
- [43] Campos Rodríguez CE, Escobar Palacio JC, Venturini OJ, Silva Lora EE, Cobas VM, Marques dos Santos D, *et al.* Exergetic and economic comparison of ORC and Kalina cycle for low temperature enhanced geothermal system in Brazil. *Appl Therm Eng.* 2013; 52: 109-19. <https://doi.org/10.1016/j.applthermaleng.2012.11.012>
- [44] Yang H, Xu C, Yang B, Yu X, Zhang Y, Mu Y. Performance analysis of an Organic Rankine Cycle system using evaporative condenser for sewage heat recovery in the petrochemical industry. *Energy Convers Manag.* 2020; 205: 112402. <https://doi.org/10.1016/j.enconman.2019.112402>
- [45] Mosaffa AH, Farshi LG, Infante Ferreira CA, Rosen MA. Exergoeconomic and environmental analyses of CO₂/NH₃ cascade refrigeration systems equipped with different types of flash tank intercoolers. *Energy Convers Manag.* 2016; 117: 442-53. <https://doi.org/10.1016/j.enconman.2016.03.053>
- [46] Mosaffa AH, Mokarram NH, Farshi LG. Thermo-economic analysis of combined different ORCs geothermal power plants and LNG cold energy. *Geothermics.* 2017; 65: 113-25. <https://doi.org/10.1016/j.geothermics.2016.09.004>
- [47] Liu Q, Duan Y, Yang Z. Effect of condensation temperature glide on the performance of organic Rankine cycles with zeotropic mixture working fluids. *Appl Energy.* 2014; 115: 394-404. <https://doi.org/10.1016/j.apenergy.2013.11.036>

- [48] Hærvig J, Sørensen K, Condra TJ. Guidelines for optimal selection of working fluid for an organic Rankine cycle in relation to waste heat recovery. *Energy*. 2016; 96: 592-602. <https://doi.org/10.1016/j.energy.2015.12.098>
- [49] Tchanche BF, Papadakis G, Lambrinos G, Frangoudakis A. Fluid selection for a low-temperature solar organic rankine cycle. *Appl Therm Eng*. 2009; 29: 2468-76. <https://doi.org/10.1016/j.applthermaleng.2008.12.025>
- [50] Darvish K, Ehyaei M, Atabi F, Rosen M. Selection of optimum working fluid for organic rankine cycles by exergy and exergy-economic analyses. *Sustainability*. 2015; 7: 15362-83. <https://doi.org/10.3390/su71115362>